

Electronic Supplementary Information (SI)

Abbreviations

- 1, [Co(pydm)₂](mdnbz)₂, C₃₀H₂₈CoN₆O₁₆, methylated counter anion mdnbz – 3,5-dinitro-4-methylbenzoate(1–)
- 2, [Co(pydm)₂](dnbz)₂, C₂₈H₂₄CoN₆O₁₆, demethylated counter anion dnbz – 3,5-dinitrobenzoate(1–); [Valigura, D.; Rajnák, C.; Moncol, J.; Titiš, J.; Boča, R. A mononuclear Co(II) complex formed from pyridinedimethanol with manifold slow relaxation channels. *Dalton Trans.* **2017**, *46*, 10950-10956.]
- 3, [Co_{0.8}Zn_{0.2}(pydm)₂](mdnbz)₂, C₃₀H₂₈Co_{0.8}N₆O₁₆Zn_{0.2}
- 3', undefined material
- 4, [Zn(pydm)₂](mdnbz)₂, C₃₀H₂₈ZnN₆O₁₆

Chemicals and handling

All chemicals were purchased and used as received in reagent grade. The manipulations were made under air conditions. The products were filtered over the ash less paper and fritted glass with porosity no. 4.

Physical Measurements

Elemental analyses were measured by Flash 2000 CHNS apparatus (Thermo Scientific). The Nujol absorption UV-Vis spectra (190 - 1100 nm) for solid samples were measured by Specord 250 Plus (Analytika Jena) with the DAD detector at room temperature.

Synthesis of 1

Co(OAc)₂·4H₂O (1 mmol, 0.249 g) was dissolved in 20 cm³ water and 2,6-dimethanolpyridine (2 mmol, 0.278 g) was washed down with another 10 cm³ of water. Mixture was stirred for 10 min at ambient temperature and 4-methyl-3,5-dinitrobenzoic acid (2 mmol, 0.452 g) and 10 cm³ water were added. Resulting mixture was stirred for 3 hours at 60°C due to worse solubility of benzoic acid in water at room temperature. Filtration was necessary. Light pink crystals were grown at room temperature and after three weeks collected. Relative yield 10%. FT-IR bands (ATR), v/cm⁻¹: 3086(w), 2443(w), 1589(m), 1530(s), 1470(m), 1443(m), 1380(m), 1342(s), 1236(m), 1146(m), 1088(m), 1023(s), 994(w), 928(w), 902(m), 793(s), 744(s), 722(s), 699(w), 667(m), 620(m), 523(w), 484(m) (s- strong, m-medium, w-weak). UV/Vis (Nujol) v_{max}/10³ cm⁻¹ (relat. absorb.): 10.75 (0.143); 20.70 (0.192). Elemental analysis C₃₀H₂₈CoN₆O₁₆ (787.51 g·mol⁻¹) found: N 10.6, C 45.6, H 3.4, calc.: N 10.7, C 45.8, H 3.6 %.

Synthesis of 3 and 3'

According to the preparation steps of **1**, three zinc-doping experiments were made. Co(OAc)₂·4H₂O and Zn(OAc)₂·2H₂O were used in molar ratios Co:Zn as 0.5 mmol/0.5 mmol (for **3**) and 0.2 mmol/0.8 mmol (for **3'**) respectively. Light pink (**3**) and white-off (**3'**) crystals were collected after three weeks. The exact content Co:Zn has been determined by the single crystal X-ray structure analysis (see below). Despite of selected ratio in the complex **3'** (also 0.1 mmol/0.9 mmol Co:Zn) doping experiment failed and bring only a small amount of undefined material many times. Yield: 13% (**3**) and 0.2 % (**3'**).

Data for **3**: FT-IR bands (ATR), v/cm⁻¹: 2441(w), 1588(m), 1530(s), 1470(m), 1442(m), 1380(m), 1341(s), 1237(w), 1164(m), 1088(w), 1024(s), 994(w), 926(w), 902(w), 793(s), 744(s), 721(s), 699(w), 665(m), 620(m), 523(w), 484(s) (s- strong, m-medium, w-weak). UV/Vis (Nujol) v_{max}/10³ cm⁻¹ (relat. absorb.): 11.19 (0.093); 21.28 (0.134). Elemental analysis for C₃₀H₂₈Co_{0.8}N₆O₁₆Zn_{0.2} (788.78 g·mol⁻¹) found: N 10.7, C 46.8, H 3.2, calc.: N 10.7, C 45.7, H 3.6%.

Data for **3'**: FT-IR bands (ATR), v/cm⁻¹: 3629(w), 1602(w), 1537(s), 1478(w), 1391(s), 1346(s), 1204(w), 1090(w), 1048(w), 923(w), 906(w), 800(m), 789(m), 743(m), 720(s), 704(w), 689(w), 618(w), 556(w), 518(w), 471(w), 444(w), 436(w), 421(m) (s- strong, m-medium, w-weak).

Synthesis of 4

Zn(OAc)₂·2H₂O (1 mmol, 0.215 g) was dissolved in 20 cm³ water and 2,6-dimethanolpyridine (2 mmol, 0.278 g) was washed down with another 10 cm³ of water. Mixture was stirred for 10 min at ambient temperature and 4-methyl-3,5-dinitrobenzoic acid (2 mmol, 0.452 g) and 10 cm³ water were added. Resulting mixture was stirred for 3 hours at 60°C. White-off crystalline product was filtered after three weeks. Relative

yield 6 %. FT-IR bands (ATR), ν/cm^{-1} : 3086(w), 2868(w), 2737(w), 2625(w), 2443(w), 1589(m), 1530(s), 1470(m), 1439(m), 1381(m), 1342(s), 1239(m), 1211(w), 1166(m), 1088(m), 1036(s), 994(w), 926(w), 902(m), 793(s), 780(w), 744(m), 721(s), 699(w), 667(m), 619(m), 525(m), 481(m) (s- strong, m-medium, w-weak). UV/Vis (Nujol) $\nu_{\text{max}}/10^3 \text{ cm}^{-1}$ (relat. absorb.): > 25. Elemental analysis for $\text{C}_{30}\text{H}_{28}\text{ZnN}_6\text{O}_{16}$; 793.95 g·mol⁻¹; found: N 10.5, C 46.3, H 3.2, calc.: N 10.6, C 45.4, H 3.5 %.

IR spectra

The samples for FT-IR (ATR) measurements were used as freshly grown crystals with no drying process.

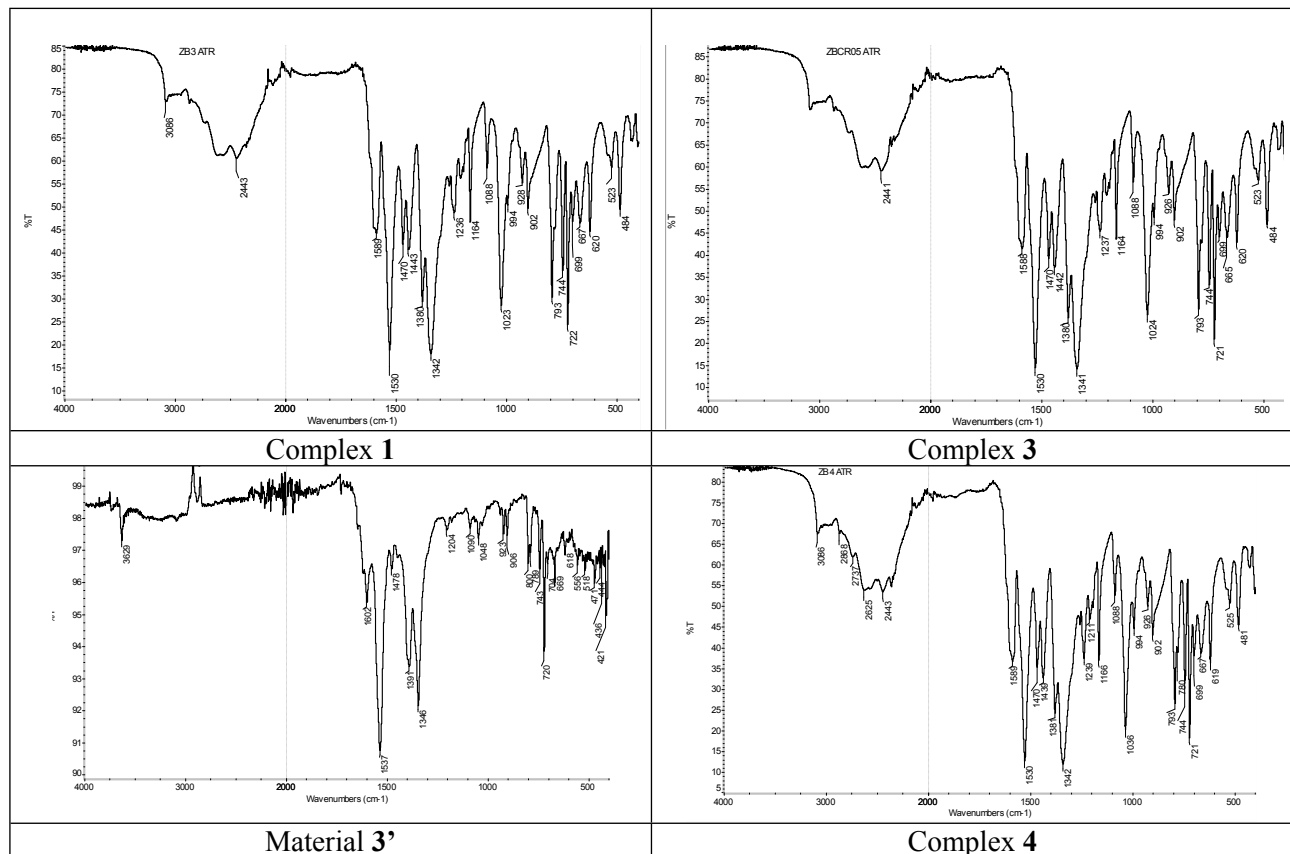


Figure S1. IR spectra for **1**, **3**, **3'**, and **4**.

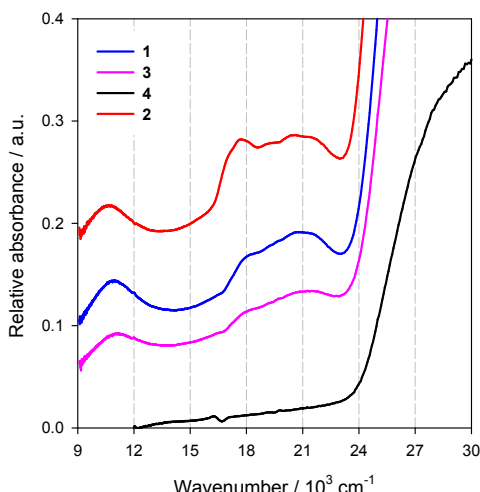


Figure S2. UV/Vis electronic spectra taken in the Nujol suspension.

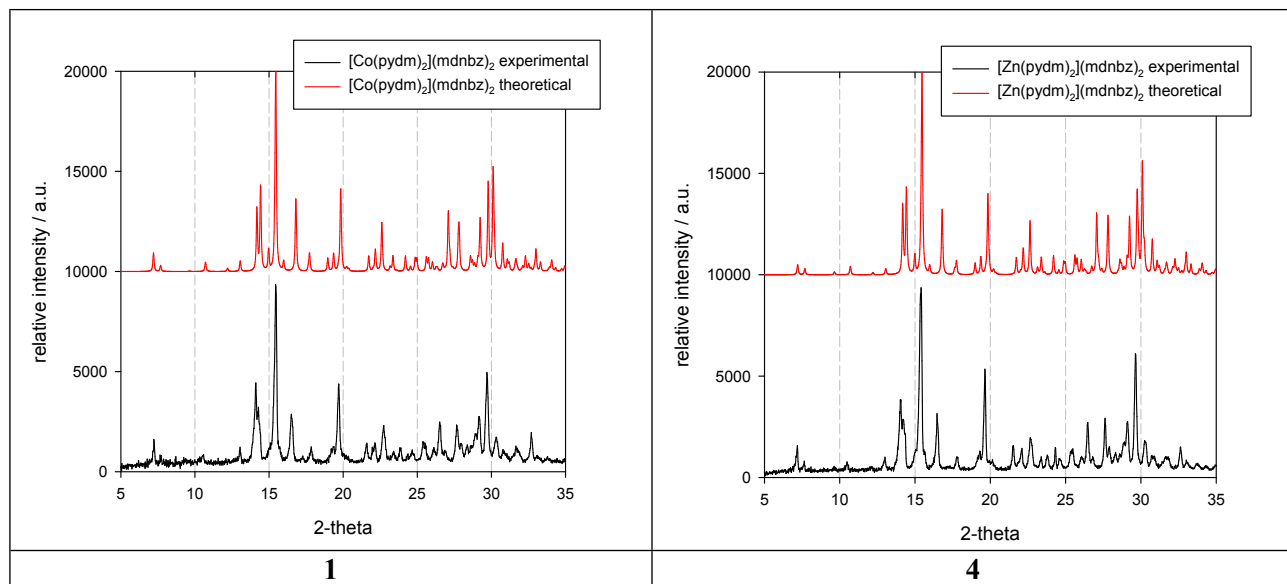


Figure S4. Powder X-ray diffraction data.

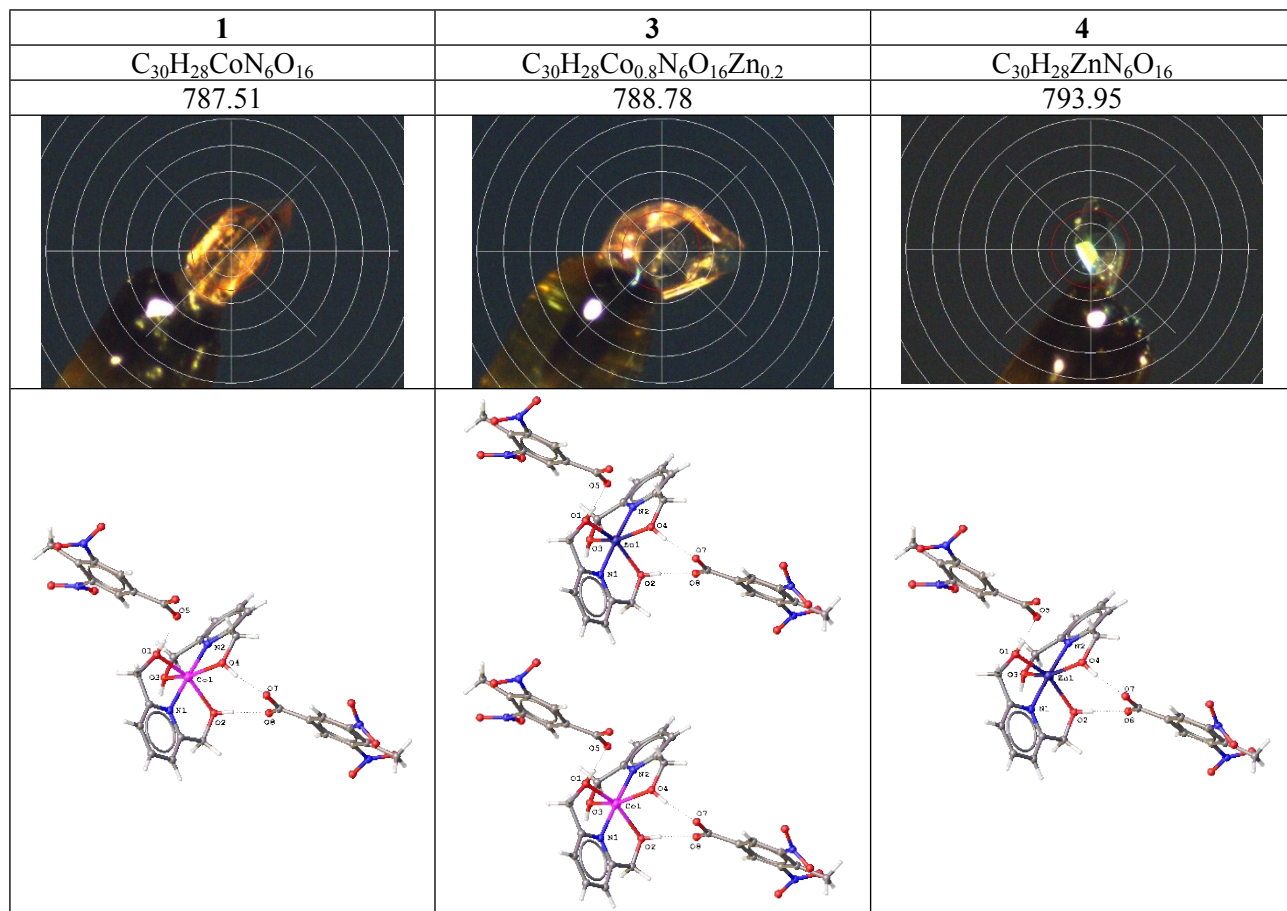


Figure S5. Single crystals mounted on the thorn in the measuring space of X-ray diffractometer.

X-ray structure determination

Table S1. Crystal data and structure refinement for **1**, **3**, **4**

	1	3	4
Empirical formula	C ₃₀ H ₂₈ CoN ₆ O ₁₆	C ₃₀ H ₂₈ Co _{0.8} N ₆ O ₁₆ Zn _{0.2}	C ₃₀ H ₂₈ ZnN ₆ O ₁₆
Formula weight	787.51	788.78	793.95
Temperature/K	100	100	100
Crystal system	monoclinic	monoclinic	monoclinic
Space group	C2/c	C2/c	C2/c
a/Å	27.2275(6)	27.2147(9)	27.3034(9)
b/Å	16.8312(5)	16.8283(7)	16.8405(8)
c/Å	14.5288(3)	14.5231(6)	14.4655(6)
$\alpha/^\circ$	90	90	90
$\beta/^\circ$	101.280(2)	101.134(3)	101.163(3)
$\gamma/^\circ$	90	90	90
Volume/Å ³	6529.5(3)	6526.1(4)	6525.4(5)
Z	8	8	8
$\rho_{\text{calc}}/\text{g/cm}^3$	1.602	1.606	1.616
μ/mm^{-1}	4.903	4.301	1.828
F(000)	3240.0	3245.0	3264.0
Crystal size/mm ³	0.2 × 0.16 × 0.16	0.23 × 0.19 × 0.16	0.14 × 0.1 × 0.1
Radiation	CuKα ($\lambda = 1.54186$)	CuKα ($\lambda = 1.54186$)	CuKα ($\lambda = 1.54186$)
2θ range for data collection/°	6.208 to 143.276	6.208 to 143.502	6.2 to 143.818
Index ranges	-24 ≤ h ≤ 33, -18 ≤ k ≤ 20, -15 ≤ l ≤ 17	-33 ≤ h ≤ 26, -20 ≤ k ≤ 18, -17 ≤ l ≤ 13	-33 ≤ h ≤ 24, -20 ≤ k ≤ 17, -13 ≤ l ≤ 17
Reflections collected	35970	33310	35121
Independent reflections	6181 [R _{int} = 0.0397, R _{sigma} = 0.0339]	6225 [R _{int} = 0.0516, R _{sigma} = 0.0404]	6207 [R _{int} = 0.0484, R _{sigma} = 0.0386]
Data/restraints/parameters	6181/85/506	6225/85/507	6207/85/507
Goodness-of-fit on F ²	1.018	1.056	1.068
Final R indexes [I>=2σ (I)]	R ₁ = 0.0424, wR ₂ = 0.0881	R ₁ = 0.0591, wR ₂ = 0.1393	R ₁ = 0.0700, wR ₂ = 0.1581
Final R indexes [all data]	R ₁ = 0.0620, wR ₂ = 0.0965	R ₁ = 0.0890, wR ₂ = 0.1593	R ₁ = 0.0916, wR ₂ = 0.1688
Largest diff. peak/hole / e Å ⁻³	0.73/-0.52	1.05/-0.78	0.70/-0.79
CCDC no.	1945478	1945479	1945480

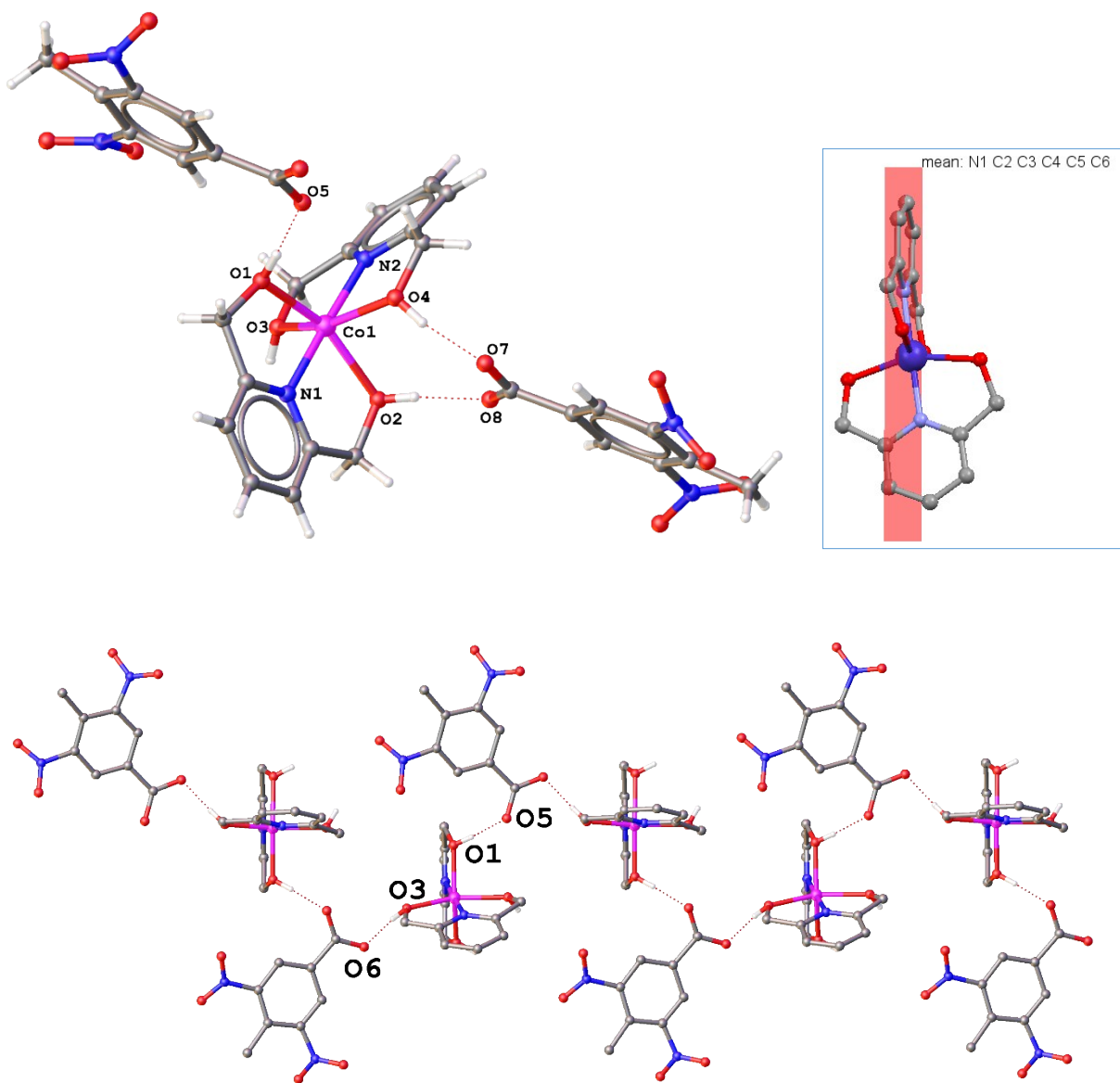


Figure S6. Labelling of atoms for the identification of metal-ligand and hydrogen bonds in **1**. The crystal structure contains supramolecular chains. SHAPE agreement factor for OC-6 is 3.20.

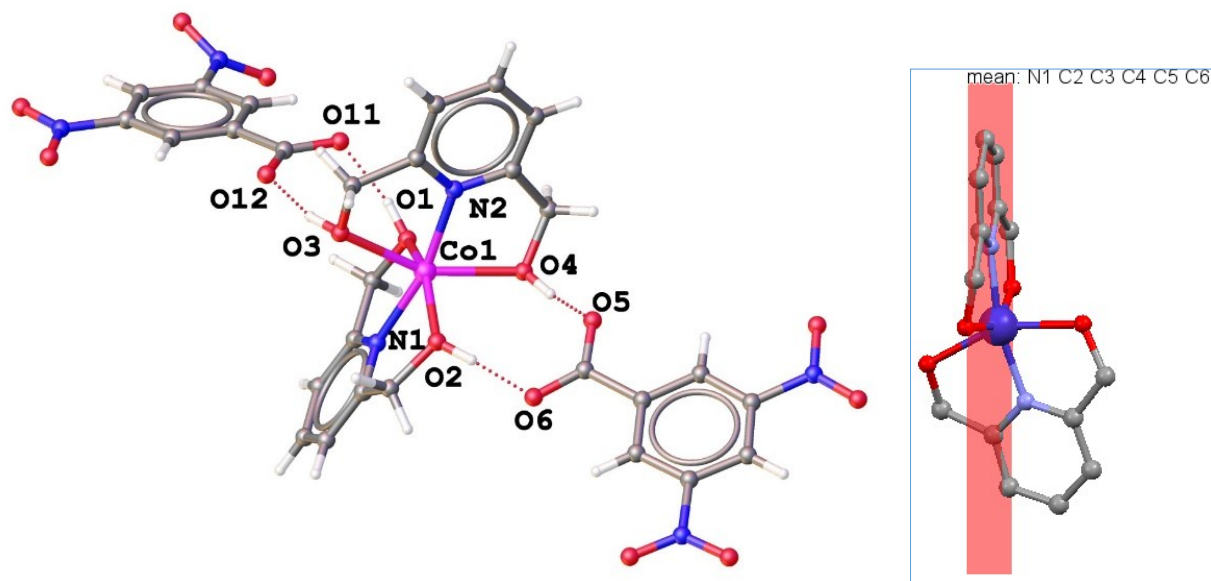


Figure S7. Labelling of atoms for the identification of metal-ligand and hydrogen bonds in **2**. The crystal structure does not contain supramolecular chains. SHAPE agreement factor for OC-6 is 4.30; GIBFIF by D. Valigura, C. Rajnák, J. Moncol, J. Titiš, R. Boča, *Dalton Trans.*, 2017, **46**, 10950.

Table S2. Selected bond lengths (\AA) and bond angles ($^\circ$) in the chromophore $\{\text{M}\text{N}_2\text{O}_4\}$

	1 (M = Co)	3 (M = $\text{Co}_{0.8}/\text{Zn}_{0.2}$)	4 (M = Zn)	2
M1–O1	2.123(2)	2.136(3)	2.157(3)	2.146(1)
M1–O2	2.117(2)	2.132(3)	2.164(3)	2.078(1)
M1–O3	2.085(2)	2.091(3)	2.105(3)	2.185(1)
M1–O4	2.144(2)	2.159(3)	2.182(3)	2.158(1)
M1–N1	2.041(2)	2.035(3)	2.037(4)	2.036(2)
M1–N2	2.035(2)	2.033(3)	2.029(4)	2.040(2)
O1–M1–O2	154.57(7)	154.89(10)	155.36(14)	
O1–M1–O3	98.69(7)	97.47(10)	94.96(13)	
O1–M1–O4	90.26(7)	90.46(10)	90.97(13)	
O2–M1–O3	92.09(7)	92.27(11)	92.89(13)	
O2–M1–O4	89.40(7)	90.22(10)	91.55(13)	
O3–M1–O4	155.19(7)	155.30(10)	155.40(13)	
N1–M1–O1	77.56(8)	77.58(11)	77.74(15)	
N1–M1–O2	77.65(8)	77.68(11)	77.69(15)	
N1–M1–O3	102.57(8)	103.28(12)	104.68(15)	
N1–M1–O2	101.93(7)	101.26(11)	99.92(14)	
N2–M1–O1	103.93(8)	104.20(11)	104.68(15)	
N2–M1–O2	100.79(8)	100.43(11)	99.80(15)	
N2–M1–O3	78.06(8)	78.12(12)	77.91(15)	
N2–M1–O4	77.34(8)	77.25(12)	77.49(14)	
N1–M1–N2	178.31(9)	177.64(13)	176.40(17)	

Table S3 Hydrogen bonds in **1**, **3**, **4**

D–H···O	d(D–H)/ \AA	d(H–A)/ \AA	d(D–A)/ \AA	D–H–A/ $^\circ$	Symmetry
1					
O1–H1···O5	0.84	1.71	2.553(2)	176	
O2–H2···O8	0.84	1.71	2.545(2)	170	
O3–H3···O6	0.84	1.74	2.561(3)	166	+x, 1–y, 1/2+z
O4–H4···O7	0.84	1.74	2.576(2)	170	
C5–H5···O6	0.95	2.46	3.285(3)	146	1–x, 1–y, 1–z
C10–H10···O8	0.95	2.52	3.397(3)	154	1/2–x, 1/2–y, 1–z
C14–H14A···O11	0.99	2.45	3.361(3)	154	+x, 1–y, –1/2+z
C14–H14B···O5	0.99	2.68	3.403(3)	131	
C21–H21···O1	0.95	2.62	3.423(3)	143	+x, 1–y, –1/2+z
3					
O1–H1···O5	0.84	1.71	2.554(4)	177	
O2–H2···O8	0.84	1.72	2.550(4)	171	
O3–H3···O6	0.84	1.74	2.564(4)	166	+x, 1–y, 1/2+z
O4–H4···O7	0.84	1.74	2.576(4)	171	
C5–H5···O6	0.95	2.46	3.278(5)	145	1–x, 1–y, 1–z
C10–H10···O8	0.95	2.51	3.393(5)	154	1/2–x, 1/2–y, 1–z
C14–H14A···O11	0.99	2.45	3.362(5)	154	+x, 1–y, –1/2+z
C14–H14B···O5	0.99	2.68	3.394(5)	129	
C21–H21···O1	0.95	2.61	3.416(4)	142	+x, 1–y, –1/2+z
4					
O1–H1···O5	0.84	1.71	2.554(4)	177	
O2–H2···O8	0.84	1.72	2.550(4)	171	
O3–H3···O6	0.84	1.74	2.564(4)	166	+x, 1–y, 1/2+z
O4–H4···O7	0.84	1.74	2.576(4)	171	
C5–H5···O6	0.95	2.46	3.278(5)	145	1–x, 1–y, 1–z
C10–H10···O8	0.95	2.51	3.393(5)	154	1/2–x, 1/2–y, 1–z
C14–H14A···O11	0.99	2.45	3.362(5)	153	+x, 1–y, –1/2+z
C14–H14B···O5	0.99	2.68	3.394(5)	129	
C21–H21···O1	0.95	2.61	3.416(4)	142	+x, 1–y, –1/2+z

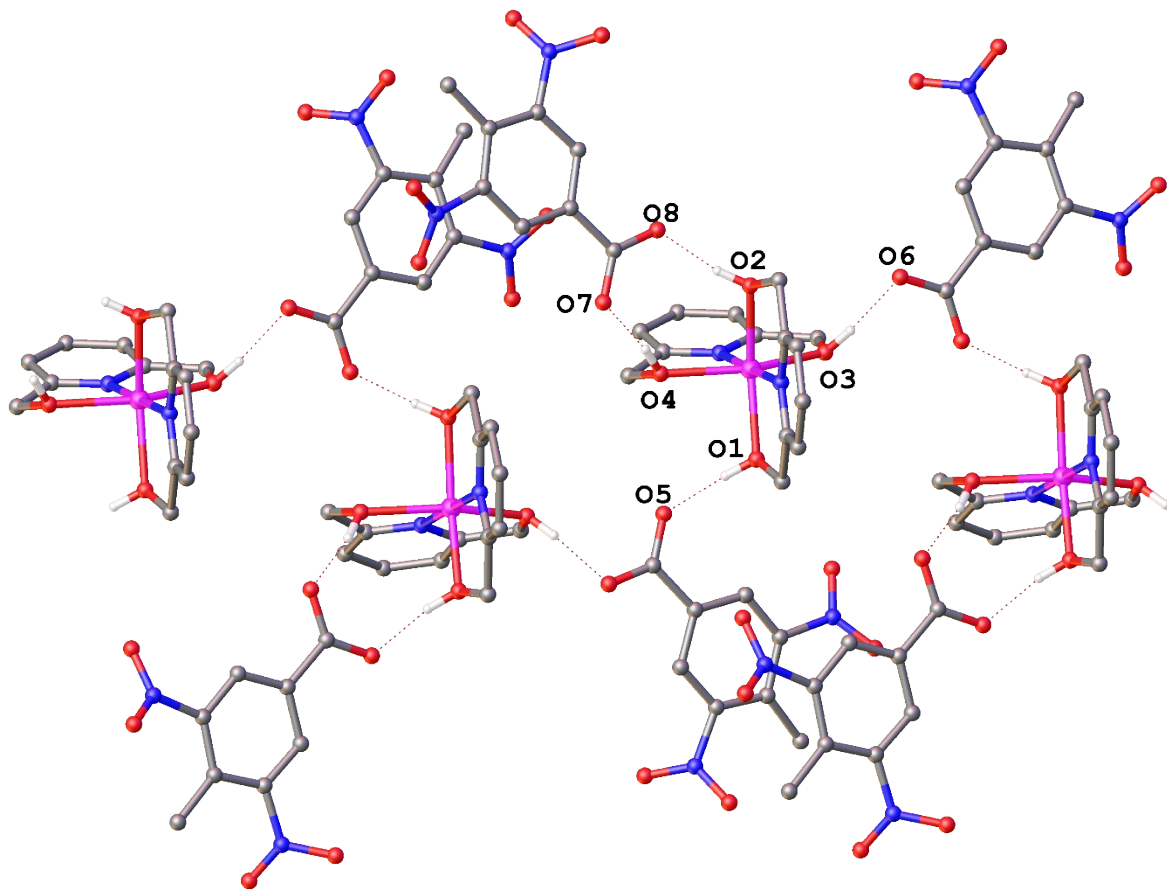


Figure S8. The supramolecular chains from ions connected through O–H···O hydrogen bonds in crystal structure of **1**.

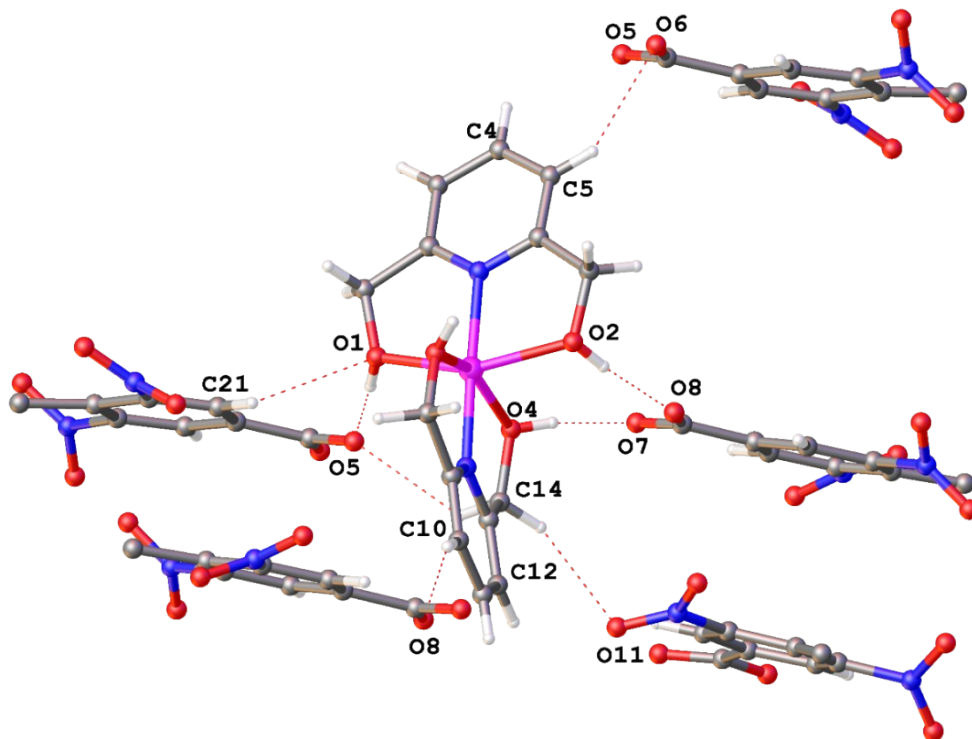


Figure S9. The O–H···O and C–H···O hydrogen bonds in crystal structure of **1**.

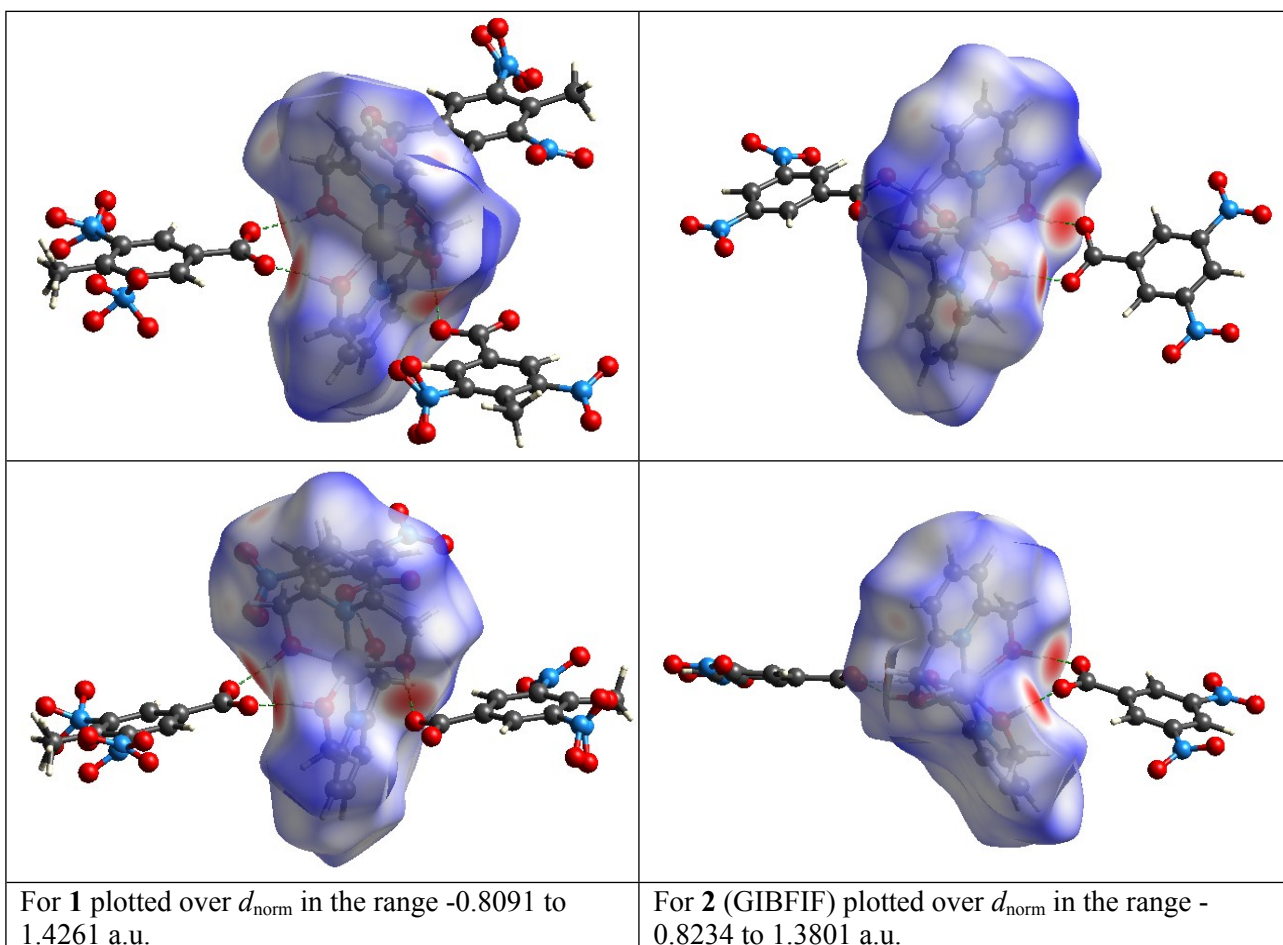


Figure S10. View of the three-dimensional Hirshfeld surface.

In Hirshfeld surface analysis, d_{norm} surface was used to study the surface characteristics and identification of close intermolecular interactions. The deep red spots on the d_{norm} Hirshfeld surface indicate the close-contact interactions, which are mainly responsible for the indicating intermolecular hydrogen bonding interactions. The 2D fingerprints plots in conjugation with the Hirshfeld surface analysis provided a quantitative description of the nature and type of intermolecular interactions apart from O–H···O and C–H···O hydrogen bonds that forming 2D supramolecular structure.

- The 2D fingerprints plots of **1** show H···H, H···O/O···H, H···C/C···H, H···H, C···C and H···N/N···H intermolecular interactions with percent contributions of 46.3, 9.0, 35.1, 5.5 and 2.3%, respectively (Fig. S11).
- The similar results for doped analogue complex and zinc analogues of complex **1** are shown in supplementary Figs. S12 and S13.
- The 2D fingerprints plots of **2** show H···H, H···O/O···H, H···C/C···H, H···H, C···C and H···N/N···H intermolecular interactions with percent contributions of 39.6, 12.9, 37.5, 2.9 and 3.2%, respectively (Fig. S14).

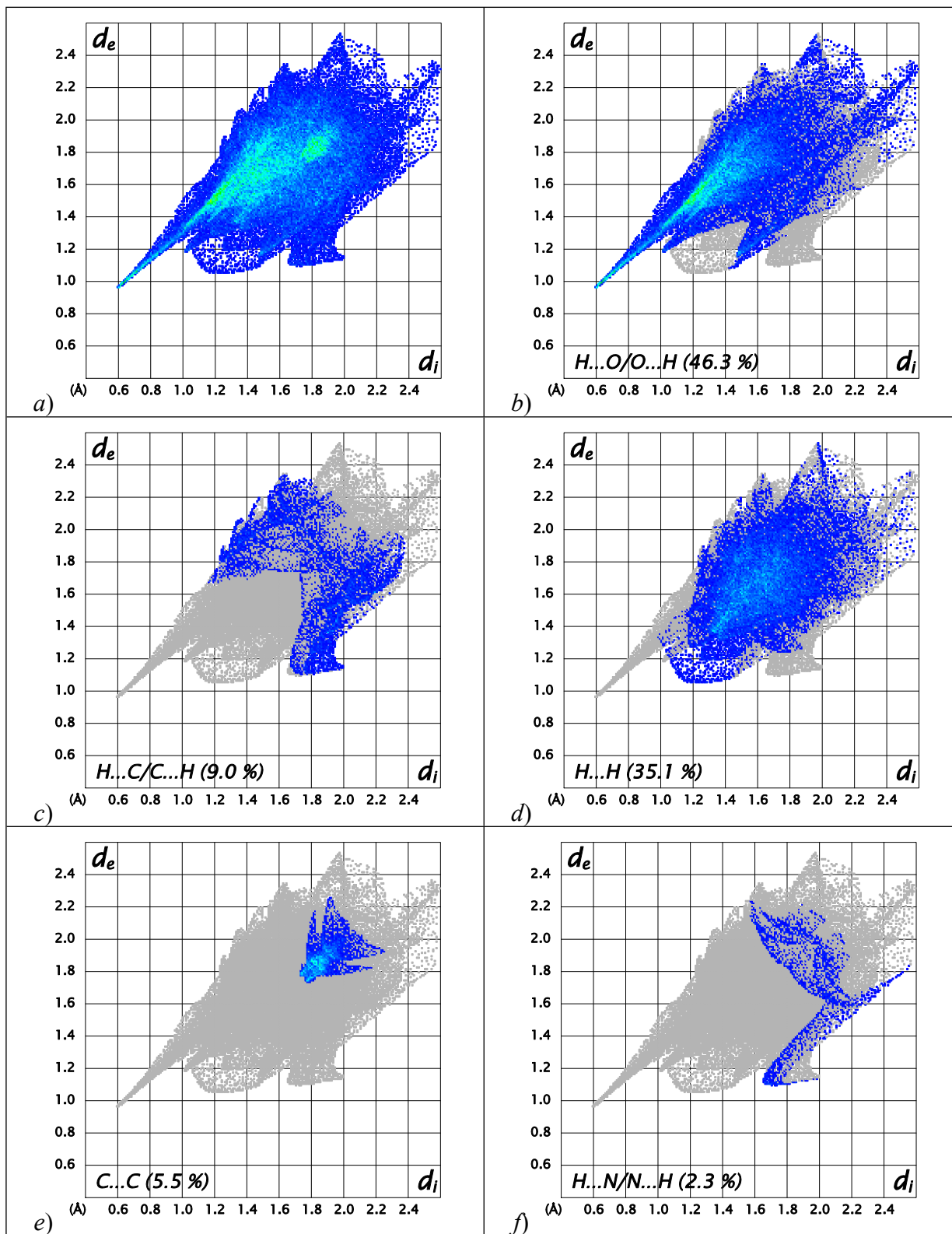


Figure S11. The full two-dimensional fingerprint plots of **1**, showing (a) all interactions, (b) $H\cdots O/O\cdots H$, (c) $H\cdots C/C\cdots H$, (d) $H\cdots H$, (e) $C\cdots C$, and (f) $H\cdots N/N\cdots H$ interactions. The d_i and d_e values are the closest internal and external distances from given on the Hirshfeld surface contacts.

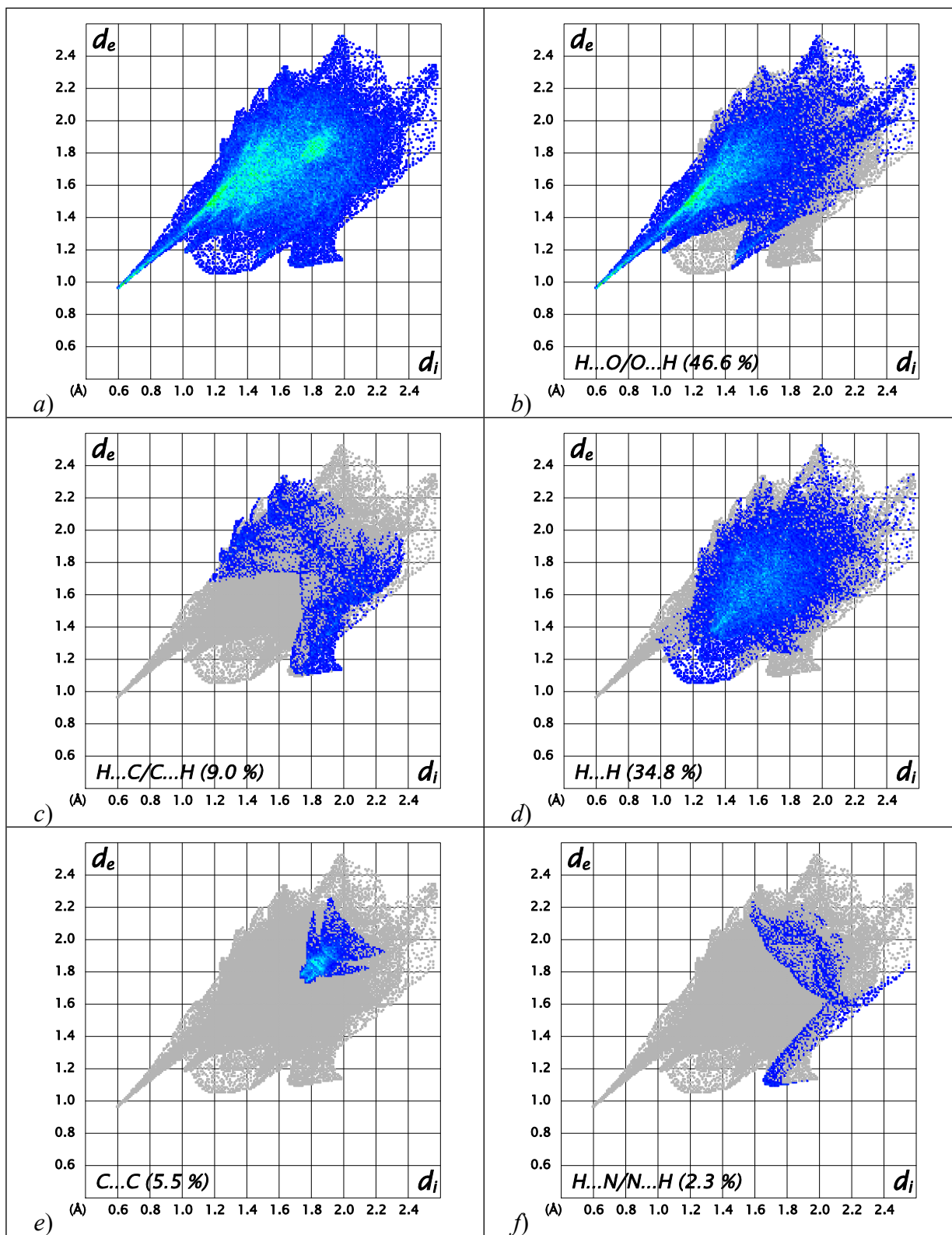


Figure S12. The full two-dimensional fingerprint plots of **3**, showing (a) all interactions, (b) $H\cdots O/O\cdots H$, (c) $H\cdots C/C\cdots H$, (d) $H\cdots H$, (e) $C\cdots C$, and (f) $H\cdots N/N\cdots H$ interactions. The d_i and d_e values are the closest internal and external distances from given on the Hirshfeld surface contacts.

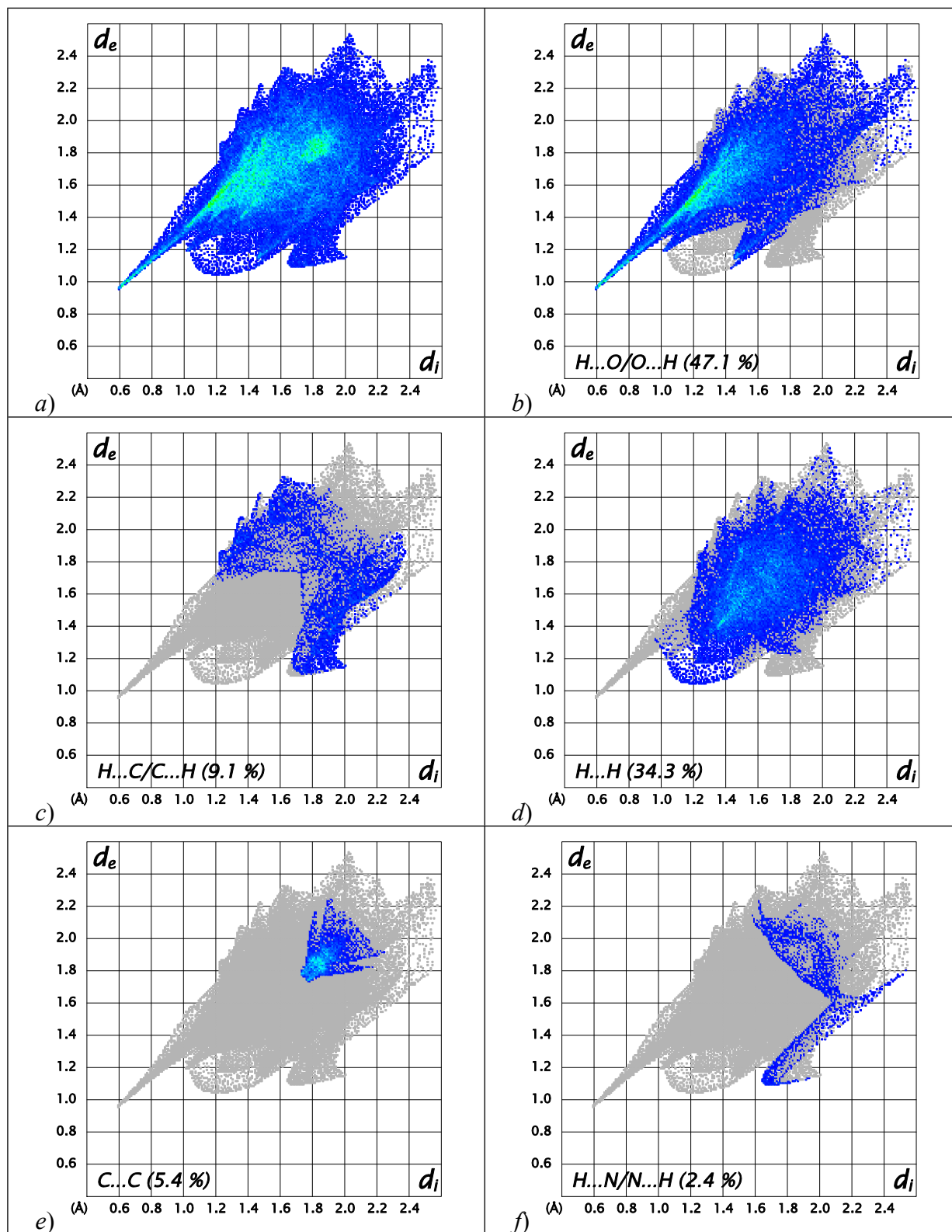


Figure S13. The full two-dimensional fingerprint plots of **4**, showing (a) all interactions, (b) $H\cdots O/O\cdots H$, (c) $H\cdots C/C\cdots H$, (d) $H\cdots H$, (e) $C\cdots C$, and (f) $H\cdots N/N\cdots H$ interactions. The d_i and d_e values are the closest internal and external distances from given on the Hirshfeld surface contacts.

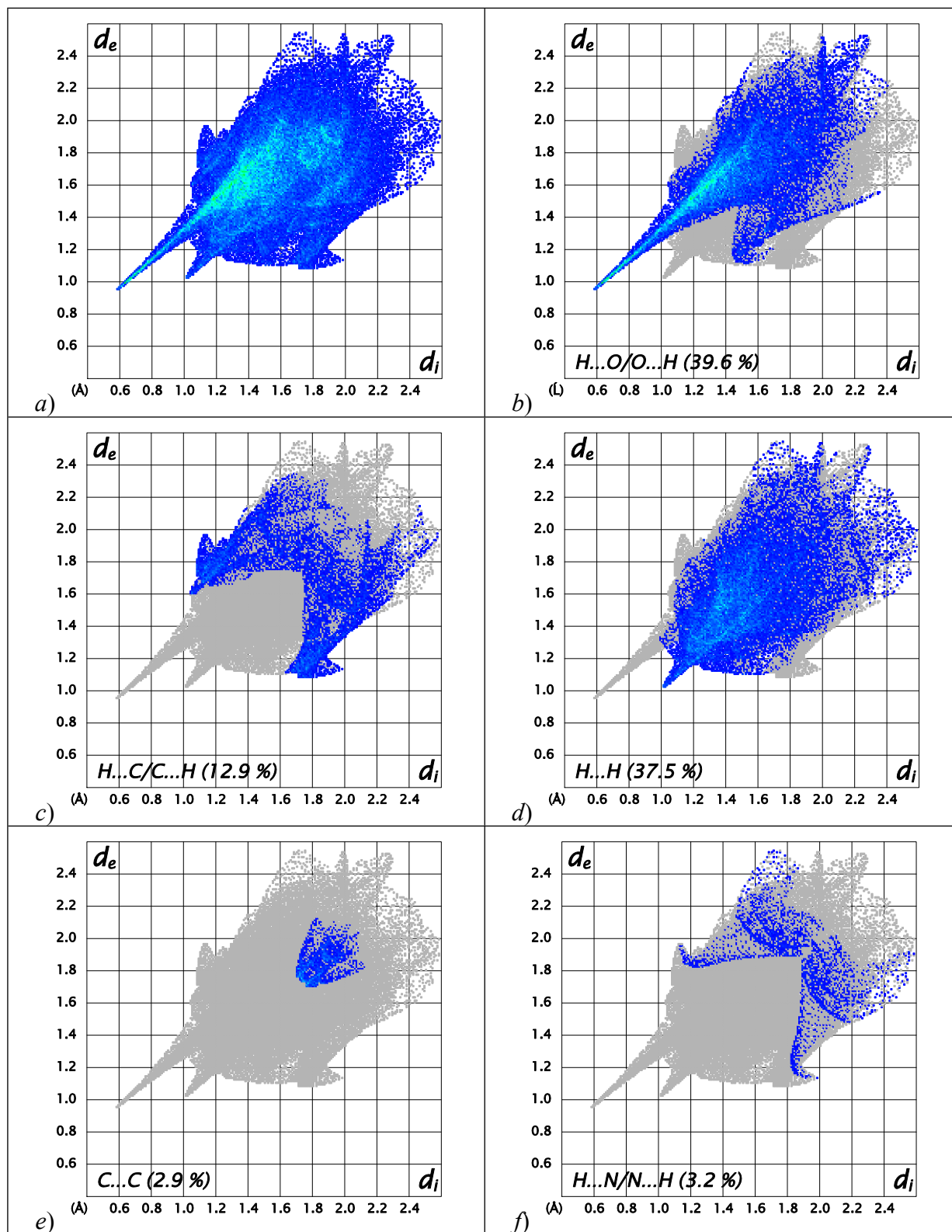


Figure S14. The full two-dimensional fingerprint plots of **2** (GIBFIF), showing (a) all interactions, (b) $H\cdots O/O\cdots H$, (c) $H\cdots C/C\cdots H$, (d) $H\cdots H$, (e) $C\cdots C$, and (f) $H\cdots N/N\cdots H$ interactions. The d_i and d_e values are the closest internal and external distances from given on the Hirshfeld surface contacts.

Table S4. Temperature dependence of AC susceptibility parameters for **1** at $B_{DC} = 0.25$ T.

T/K	$R(\chi')$ %/	$R(\chi'')$ %	χ_{LF}	α_{LF}	τ_{LF} $/10^{-3}$ s	χ_{IF}	α_{IF}	τ_{IF} $/10^{-3}$ s	χ_{HF}	α_{HF}	τ_{HF} $/10^{-6}$ s	x_{LF}	x_{IF}	x_{HF}
1.9	0.78	2.9	1.8(2)	.18(6)	282(28)	6.2(8)	.21(5)	3.1(4)	9.8(1)	.34(5)	164(63)	.19	.45	.37
2.3	0.35	2.1	1.0(1)	.18(4)	282(19)	4.6(8)	.12(4)	1.9(1)	8.4(1)	.38(4)	188(86)	.12	.43	.45
2.7	0.28	1.4	0.56(4)	.12(4)	308(21)	3.9(6)	.06(3)	1.1(1)	7.2(1)	.34(4)	128(44)	.08	.47	.45
3.1	0.52	0.94	0.33(4)	.08(8)	329(42)	4.0(8)	.03(4)	0.54(4)	6.3(1)	.24(12)	66(37)	.05	.58	.37
3.5	0.58	0.74	0.18(3)	.03	375(74)	4.2(4)	.03(2)	0.25(2)	5.6(1)	.01	29(9)	.03	.72	.25
3.9	0.26	1.0	0.10(1)	.00	371(59)	3.8(23)	.02	0.13(3)	5.1(1)	.01	20(28)	.02	.72	.26
4.3	0.41	4.0				4.6(1)	.05(1)	0.048(1)					1	
4.7	0.29	2.6				4.3(1)	.04(1)	0.027(1)					1	
5.1	0.24	2.8				3.9(1)	.03(1)	0.015(1)					1	

^a Obtained by a three-set (single-set) Debye model; χ in units of 10^{-6} m³ mol⁻¹; adiabatic susceptibility $\chi_s = 0$.

Table S5. Comparison of Mulliken charges (B3LYP/ZORA-TZVPP) on oxygen atoms for methylated and demethylated counter anions.

	<i>dnbz</i>	<i>mdnbz</i>
O1	-0.4763	-0.4772
O2	-0.4759	-0.4772
O3	-0.3171	-0.3120
O4	-0.3379	-0.3298
O5	-0.3172	-0.3120
O6	-0.3378	-0.3290

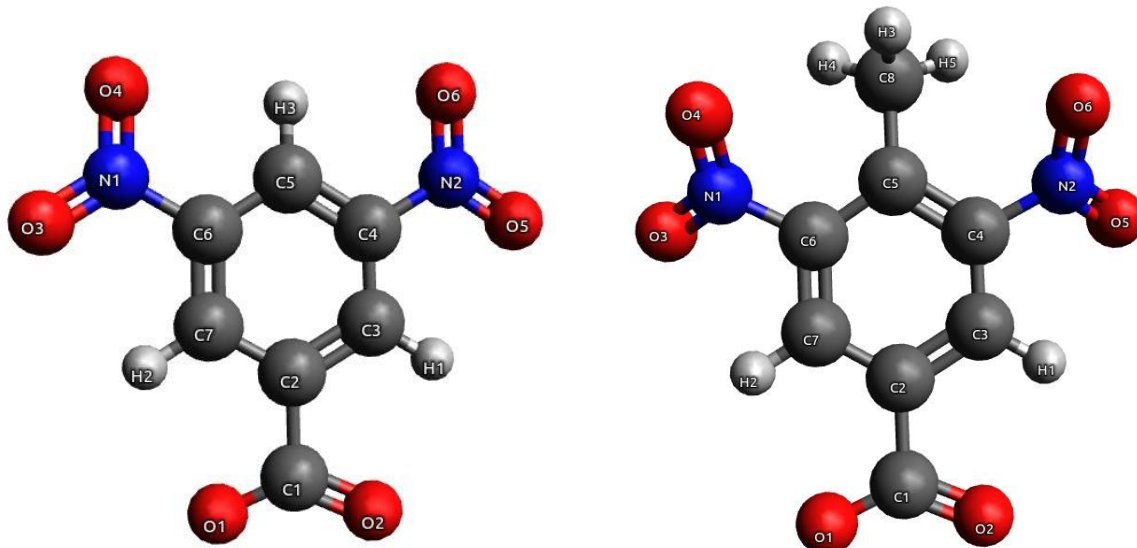


Figure S15. Optimized structures (BP86-D3/ ZORA-TZVP) of the *dnbz* and *mdnbz* counter anions. Note: DFT calculations of Mulliken charges for two optimized (BP86-D3/ ZORA-TZVP) anions *dnbz* and *mdnbz* have been done at B3LYP/ZORA-TZVPP level of theory using ORCA package.

Table S6. Ab initio calculations (CASSCF/NEVPT2). Quartet-to-quartet transition energies (ΔE_i) and spin-orbit multiplets (ΔE_i^{soc}) as well as individual contributions to the ZFS parameters (D_i and E_i).

$\Delta E_i / \text{cm}^{-1}$	D_i / cm^{-1}	E_i / cm^{-1}	$\Delta E_i^{\text{soc}} / \text{cm}^{-1}$
0 (${}^4\text{E}_g$), 707.6	0, -86.897	0, 0.020	0
1831.5 (${}^4\text{A}_{2g}$)	11.695	-11.760	145.2
7941.4	5.056	5.883	870.0
8128.1	3.957	-2.327	1098.7
11688.5	0.154	0.309	2055.7
19141.7	0.033	-0.023	2174.8
19782.3	0.011	-0.011	
23970.7	0.059	-0.058	
24204.1	-0.076	0.006	